

Document downloaded from:

<http://hdl.handle.net/10251/82755>

This paper must be cited as:

Nigar, H.; García-Baños, B.; Penaranda-Foix, FL.; Catalá Civera, JM.; Mallada, R.; Santamaria, J. (2016). Amine-functionalized mesoporous silica: A material capable of CO<sub>2</sub> adsorption and fast regeneration by microwave heating. *AIChE Journal*. 62(2):547-555. doi:10.1002/aic.15118.



The final publication is available at

<http://dx.doi.org/10.1002/aic.15118>

Copyright Wiley

Additional Information

**Amine-functionalized mesoporous silica. A material capable of CO<sub>2</sub> adsorption and fast regeneration by microwave heating**

Journal:	<i>AICHE Journal</i>
Manuscript ID:	Draft
Wiley - Manuscript type:	Research Article
Date Submitted by the Author:	n/a
Complete List of Authors:	Santamaria, Jesus; University of Zaragoza, Nanoscience Institute of Aragon and Chemical and Environmental Engineering Mallada, Reyes; Nanoscience Institute of Aragon, Chemical and Environmental Engineering Nigar, Hakan; University of Zaragoza, Nanoscience Institute of Aragon and Chemical and Environmental Engineering Garcia-Baños, Beatriz; Instituto ITACA, Catalá-Civera, Jose; Instituto ITACA, Peñaranda-Foix, Felipe; Instituto ITACA,
Keywords:	Adsorption/gas, Microwave heating, Mesoporous silica, amine functionalization, dielectric measurements

SCHOLARONE™  
Manuscripts

1  
2  
3 **Amine-functionalized mesoporous silica. A material capable of CO<sub>2</sub> adsorption**  
4  
5  
6 **and fast regeneration by microwave heating**

7  
8 **Hakan Nigar**

9  
10 Nanoscience Institute of Aragon and Chemical and Environmental Engineering

11  
12 Department, University of Zaragoza, 50018 Zaragoza, Spain

13  
14 **Reyes Mallada\*, Jesus Santamaría\***

15  
16 Nanoscience Institute of Aragon and Chemical and Environmental Engineering

17  
18 Department, University of Zaragoza, 50018 Zaragoza, Spain

19  
20 Networking Research Centre CIBER-BBN, 28029 Madrid, Spain

21  
22 **Beatriz Garcia-Baños, Felipe L. Peñaranda-Foix, Jose M. Catalá-Civera**

23  
24 Instituto ITACA, Universidad Politecnica de Valencia, Camino de Vera, 46022,

25  
26 Valencia, Spain

27  
28 \*Corresponding authors: [rmallada@unizar.es](mailto:rmallada@unizar.es), [jesus.santamaria@unizar.es](mailto:jesus.santamaria@unizar.es)

29  
30  
31  
32  
33 The surface of ordered mesoporous (MCM-48) silica has been subjected to covalent  
34 grafting with silane molecules containing one to three amino groups. The dielectric  
35 properties of the materials were studied in detail, and the functionalized materials  
36 were used for CO<sub>2</sub> adsorption at room temperature, followed by regeneration under  
37 either conventional heating or microwave irradiation. It has been found that, as the  
38 intensity of functionalization with amino groups increases (from mono to tri-amino  
39 silanes) both the CO<sub>2</sub> load and the dielectric response at microwave frequencies  
40 increase. In particular, functionalization with a tri-amino silane derivative gave the  
41 highest CO<sub>2</sub> adsorption and the fastest microwave heating, resulting in a 4-fold  
42 acceleration of adsorbent regeneration. The grafted material was fully stable for at  
43 least 20 adsorption-regeneration cycles, making it an ideal candidate for microwave-  
44 swing adsorption (MWSA) processes.  
45  
46  
47  
48  
49  
50  
51  
52  
53  
54  
55  
56  
57  
58  
59  
60

## Introduction

Among CO<sub>2</sub> capture technologies, adsorption is the most promising in the range of low temperature operation<sup>1</sup> including post-combustion capture systems as well as the capture of CO<sub>2</sub> from ambient air its subsequent reutilization as part of a climate change mitigation strategy.<sup>2</sup> Apart from the more classical zeolites and activated carbons, in recent years metal organic frameworks (MOF), and a wide variety of amino-functionalized materials have shown exciting performance in terms of loading capacity and selectivity towards CO<sub>2</sub> adsorption. At a low CO<sub>2</sub> pressure of 0.1 kPa and 293 K the highest load around 6 mmol/g (26 %wt.) has been obtained with Mg-MOF74.<sup>3</sup> However, it is important to note that this material is hydrophilic and in the presence of water its capacity is strongly reduced, this behavior also observed for most zeolites. Appropriate functionalization of adsorbents (typically by amino groups) can also be used to increase the capacity and selectivity towards CO<sub>2</sub> adsorption. In the group of amine modified mesoporous silicas, the best results were reported by the group of Sayari et al.<sup>4,5</sup> They synthesized a pore-expanded mesoporous silica (PE-MCM41) and modified it with a tri-amine silane agent. The CO<sub>2</sub> uptake at 0.1 bar and 298 K was 2.2 mmol/g (9.7 %wt.), comparable to that of a typical zeolite 13X. However, in this case the presence of water increased the CO<sub>2</sub> uptake increases (2.9 mmol/g) outperforming the zeolite.

At least as important as the capacity and selectivity of a sorbent towards CO<sub>2</sub> is the possibility of economic regeneration. Ideally, desorption processes would be fast (to produce a concentrated CO<sub>2</sub> stream) and would require a minimal amount of energy. In fact, energy costs often determine the viability of the entire process,<sup>6</sup> which has prompted an intense research into alternative methods of energy management. In the last two decades microwave (MW) irradiation, has emerged as a highly effective

1  
2  
3 way to supply energy in several types of intensified processes<sup>7</sup> including those  
4 involving solid materials<sup>8,9</sup> such as sintering and ceramic processing<sup>10</sup>, catalysis<sup>11</sup> and  
5 desorption<sup>12</sup> in the so called Microwave Swing Adsorption, MWSA process. The  
6 main advantage of MWSA relate to the fact that, unlike conventional heating where  
7 solids heat through conduction and convection, microwaves are able to provide  
8 energy to susceptible materials in a direct manner, and thus MWs can achieve the  
9 volumetric heating of adsorbent materials when they are capable of absorbing the  
10 microwave energy. Alternatively, the use of MWs may allow for direct transfer of the  
11 energy to the adsorbate without being absorbed by the adsorbent.<sup>13</sup> There is also the  
12 possibility of selective targeting of the surface itself or of its functional groups to  
13 promote microwave desorption processes.<sup>6</sup>

14  
15  
16  
17  
18  
19  
20  
21  
22  
23  
24  
25  
26  
27  
28  
29  
30  
31  
32  
33  
34  
35  
36  
37  
38  
39  
40  
41  
42  
43  
44  
45  
46  
47  
48  
49  
50  
51  
52  
53  
54  
55  
56  
57  
58  
59  
60

Widely employed MW-heatable microporous sorbents include zeolites (or zeotypes) as polar sorbents, and activated carbon as non-polar sorbents. These two classes of materials are the only ones studied so far in MWSA, being the carbon family the most frequently used. Carbon materials are good microwave absorbers as a consequence of the interactions of the delocalized  $\pi$ -electrons with the MWs, thus converting MW energy into heat.<sup>14,15</sup> In the case of zeolites, a different heating mechanism has been found<sup>16-19</sup> related to the interaction of the electromagnetic field with, i) the water or polar molecules adsorbed in the pores, ii) the hydroxyl groups on the surface and iii) the cation movement in the structure.

The ability of a material to be heated in the presence of the MW field is defined by its dielectric loss tangent:  $\tan\delta=\epsilon/\epsilon'$ . In turn, the dielectric loss tangent is composed of two parameters, the dielectric constant (or real permittivity),  $\epsilon'$ , and the dielectric loss factor (or imaginary permittivity),  $\epsilon''$ ; i.e.,  $\epsilon=\epsilon'-i\epsilon''$ , where  $\epsilon$  is the complex permittivity. The dielectric constant ( $\epsilon'$ ) determines the electric energy

1  
2  
3 storage in the dielectric, while the dielectric loss factor ( $\epsilon''$ ) measures the dissipation  
4  
5 of electric energy in form of heat within the material.<sup>9</sup> The measurement of dielectric  
6  
7 properties in solids is a difficult task, since many parameters influence the dielectric  
8  
9 properties, in particular the frequency, the humidity, the density of the solid bed and  
10  
11 specially the temperature play an important role.  
12

13  
14 Catala-Civera et al.<sup>20</sup> reported that, the dynamic measurement of dielectric  
15  
16 properties of materials simultaneously with the application of MW heating at high  
17  
18 temperatures ( $>1000^{\circ}\text{C}$ ). This report can also help to better understanding, the  
19  
20 interactions that take place during MW heating in comparison with conventional  
21  
22 heating techniques. Understanding the microwave heating behavior of materials may  
23  
24 also lead us to the most effective way of transferring the energy directly to the  
25  
26 processed materials. With proper understanding, many technically important materials  
27  
28 can be heated in a more rapid, uniform, selective, lower cost and controlled form than  
29  
30 is possible with conventional methods.<sup>8</sup>  
31  
32

33  
34 Heat-driven regeneration modes, such as Temperature Swing, TS, and  
35  
36 Temperature Swing Vacuum, TSV, are preferentially employed for the regeneration  
37  
38 of amine-containing sorbents due to the chemical  $\text{CO}_2$ -sorbent interactions. However  
39  
40 with these procedures the main drawback is that under conventional heating the  
41  
42 temperature rise of the solid is slow and rapid cycling cannot be implemented.<sup>21</sup> This  
43  
44 problem could be solved using the volumetric and selective heating afforded by  
45  
46 microwaves. In a previous work of our laboratory, we showed a reduction in  
47  
48 desorption time of 75% using MW-heatable zeolites as sorbents of n-hexane.<sup>19</sup> On the  
49  
50 other hand, the desorption of  $\text{CO}_2$  by microwaves from zeotypes (zeolite X and ETS-  
51  
52 10)<sup>6,22</sup> and carbon<sup>23</sup> has been recently reported. The promising results of these works  
53  
54 suggest that MW heating could overcome some of the main challenges in  $\text{CO}_2$  capture  
55  
56  
57  
58  
59  
60

1  
2  
3 which include affordable production of a high-purity CO<sub>2</sub> stream (high  
4 adsorption/desorption rates, low energy consumption) while preserving the textural  
5 characteristics of the sorbents<sup>6</sup> to an extent that would allow their multiple reuse.  
6  
7

8  
9  
10 In a previous work, we synthesized a mesoporous silica MCM-48 and  
11 established the optimal conditions for functionalization with a mono-amine group.<sup>24</sup>  
12 This material showed an excellent efficiency for CO<sub>2</sub> removal at low partial pressures  
13 (0.5 mmol CO<sub>2</sub>/mol N at 5 kPa), although sorbent regeneration by MW was not  
14 explored. In the present work, we have modified the same MCM-48 with silane  
15 agents containing one, two and three amino groups to increase the CO<sub>2</sub> uptake, and  
16 we have also investigated the effect of these functionalizations have on the MW  
17 absorption properties of the solid, for MWSA operation.  
18  
19  
20  
21  
22  
23  
24  
25  
26

27 In addition to studying the adsorption of CO<sub>2</sub> on mesoporous silica  
28 functionalized with different amino groups, this study will cover two important  
29 aspects in the successful design CO<sub>2</sub> MWSA processes, i.e., i) the study of the  
30 dielectric properties of the materials and ii) the regeneration process itself when  
31 carried out under microwave irradiation with especial focus on the regeneration rates  
32 achieved. Understanding MW-heating behavior of materials ultimately involves  
33 correlating dielectric properties with surface chemistry. The study will include the  
34 comparison with conventional electrical heating and the study of the stability of the  
35 sorbents after several regeneration cycles under MW-heating. In spite of the  
36 considerable potential of MWSA processes for CO<sub>2</sub> management, these aspects have  
37 been scarcely studied.<sup>22,25</sup>  
38  
39  
40  
41  
42  
43  
44  
45  
46  
47  
48  
49  
50  
51  
52  
53  
54  
55  
56  
57  
58  
59  
60

## Experimental

### *Mesoporous silica MCM-48 synthesis*

A hydrothermal method was used for the synthesis of the MCM-48 with the following molar gel composition: 1.4 SiO<sub>2</sub>: 1.0 CTABr : 0.35 Na<sub>2</sub>O : 5.0 EtOH : 140 H<sub>2</sub>O. Ludox AS40 (40% SiO<sub>2</sub> : 60% H<sub>2</sub>O, Sigma-Aldrich) was used as a silica source, CTABr (hexadecyltrimethylammonium bromide, Sigma-Aldrich) as a structure-directing agent and EtOH (Absolute, Sigma-Aldrich) as an additive for the mesophase control. Two different solutions were prepared. For the silica source solution, Ludox was added slowly drop-by-drop into an aqueous solution of 1 M NaOH under vigorous stirring, this mixture was heated up to 343 K for 1 h and then the solution was cooled to room temperature. To prepare the surfactant solution, CTABr was dissolved slowly in an EtOH/H<sub>2</sub>O mixture under gently stirring to avoid the formation of bubbles. The silica solution was added drop-by-drop into the surfactant solution and stirred for 1 h. The prepared gel with a total amount of 70 g was divided in two Teflon-lined stainless steel autoclaves and subjected to hydrothermal synthesis at 373 K in a preheated oven for 4 days. Then the solid product was filtered (medium flow rate disc filter, PRAT-DUMAS), washed with hot water and dried overnight. For the elimination of the surfactant, the solid product was calcined at 813 K with a heating rate of 1 K/min in air for 6 h.<sup>24</sup>

### *Amine functionalization*

The mono-, di-, and tri-amine silane agents (see Figure 1b ) used for grafting were 3-triethoxysilylpropylamine (98%), [3-(2-aminoethylamino)propyl]trimethoxysilane (97%), and 2-[2-(3-trimethoxysilylpropylamino)ethylamino]ethylamine (technical grade), respectively, and supplied from Sigma-Aldrich. For dry grafting, 300 mg of MCM-48 powder was dispersed in 15 mL of dry toluene in a 250 mL twin-neck



1  
2  
3 round-bottom flask under continuous stirring (400 rpm) in an Argon atmosphere  
4 during 15 min., then the flask was immersed in a temperature controlled oil bath,  
5  
6 when the mixture reached to 383 K, 650  $\mu$ L of the amine silane agent were added into  
7  
8 the flask and stirred for 1 h under reflux. Then the solid product was vacuum filtered  
9  
10 and washed with dichloromethane/diethyl ether (1:1) mixture and dried at 323 K for  
11  
12 12 h. Amine functionalized MCM-48 samples were designated as MCM-48 mono-,  
13  
14 MCM-48 di-, MCM-48 tri.

### 18 19 *Adsorption-Desorption Experiments*

20  
21 Adsorption – Desorption experiments were performed in an experimental setup  
22 previously described<sup>19</sup> which consisted of three mass flow controllers, two automatic  
23  
24 4-way valves and an on-line quadrupole mass spectrometer (OMNistar), MS, for the  
25  
26 analysis of the gases. The experimental system was computer-controlled by a  
27  
28 Labview customized program. Two different pure (99.9999%, Praxair) gases and  
29  
30 mixtures thereof containing CO<sub>2</sub> for adsorption or N<sub>2</sub> for regeneration were fed to the  
31  
32 bed at a total flow rate of 100 sccm. Adsorption experiments were done at 298 K and  
33  
34 1 bar with a 15 % concentration of CO<sub>2</sub> in a fixed-bed in a quartz tube (200 mg, 50-  
35  
36 150  $\mu$ m, L=10 mm,  $\varnothing_{in}$ =7 mm). Prior to the adsorption runs, the sample was  
37  
38 regenerated thermally while passing N<sub>2</sub> through the bed. Regeneration was carried out  
39  
40 either by conventional heating with an electrical oven or by microwave heating. The  
41  
42 microwave system (Sairem Iberica, see Figure 1 supplementary information) consists  
43  
44 of a solid state microwave generator at 2.43 to 2.47 GHz with a maximum power of  
45  
46 150 W and a TE10 mode microwave cavity (Sairem) with a WR340 waveguide. The  
47  
48 cavity was adjusted to reduce the reflected power below 5% by changing the  
49  
50 frequency. The reflected power was measured with a Network Analyzer (Agilent  
51  
52 E5061B 5 Hz – 3 GHz).  
53  
54  
55  
56  
57  
58  
59  
60

### *Temperature measurements*

The temperature in the fixed-bed was measured with an optical fiber (range: 193-523 K, Ø:1 mm, Neoptix) inside a capillary quartz tube located in the center of the fixed-bed.

To have a direct and accurate comparison of the heating rates obtained with different degrees of amination slabs consisting of a mixture (2:1) of KBr (material transparent to MW radiation) and the specific adsorbent were prepared. The slabs were located within the waveguide in front of one of the sampling windows to allow direct measurement of the temperature of the surface using an infrared thermographic camera (range: 273-873 K, InfraTec, GmbH). A scheme is provided in Figure 7.

### *Characterization techniques*

X-ray diffraction analyses were carried out using a Philips X'Pert MPD diffractometer with  $\text{CuK}\alpha$  radiation. The diffraction data were recorded in the  $2\theta$  range of  $0.6\text{--}6.5^\circ$  with a scanning rate of 5 s/step (step  $2\theta=0.02$ ).

Nitrogen adsorption isotherms were measured at 77 K on Micromeritics TriStar 3000 analyzer. Non-functionalized MCM-48 samples were degassed under vacuum at 473 K for 8 h, and the mono-, di- and tri-amine functionalized MCM-48 samples were degassed at 383 K for 10 h. BET surface areas were calculated using the BET equation in the linear range and pore volume was calculated at a relative pressure of 0.95. Pore size was analyzed with the software developed by Micromeritics based on Density Functional Theory, DFT. In particular for the analysis of mesoporous silicas the selected model to fit the experimental isotherm was the DFT- $\text{N}_2$  model, based on a cylindrical pore model with oxide surface.<sup>26</sup>

1  
2  
3 CO<sub>2</sub> adsorption isotherms of the different samples were measured at 298 K on  
4  
5 Micromeritics ASAP 2020 analyzer; fixed amounts of CO<sub>2</sub> were dosed to the sample  
6  
7 till the equilibrium pressure was achieved.  
8

9  
10 TEM images were obtained with a transmission electron microscope FEI TECNAI  
11  
12 T20, working at 200 kV. This microscope belongs to the Laboratory of Advanced  
13  
14 Microscopies, LMA, in the installations at the Institute of Nanoscience of Aragon  
15  
16 (INA), University of Zaragoza..  
17

18  
19 Thermogravimetric analysis (TGAQ5000 TA instruments with a heating rate 5 K/min  
20  
21 up to 1073 K under airflow ) was used to obtain the amount of N in the samples, using  
22  
23 the weight loss between 403 and 1073K. This method was validated in our previous  
24  
25 publication<sup>24</sup> by checking its results against those of standard methods such as the so-  
26  
27 called fluorescamine method that evaluates the amount of amino groups based in  
28  
29 reaction of the non-fluorescent fluorescamine with the primary amines, that yields a  
30  
31 fluorescent derivative. From the total weight loss between 403 K and 1073 K the  
32  
33 amount of N was calculated using the equivalence of 69, 49 and 47 mg of weight loss  
34  
35 per mmol of N, for the mono-, di- and tri- functionalized samples respectively.  
36  
37

38  
39 Fourier transform infrared (FTIR) spectroscopy of the fresh samples (not dehydrated)  
40  
41 was performed with a Bruker Vertex 70 FTIR spectrometer equipped with a DTGS  
42  
43 detector and a Golden Gate diamond ATR accessory. Spectra were recorded by  
44  
45 averaging 100 scans in the 4000–600 cm<sup>-1</sup> wave number range at a resolution of  
46  
47 2 cm<sup>-1</sup>. Data evaluation was carried out by OPUS software from Bruker Optics.  
48  
49

### 50 *Dielectric Properties*

51  
52 Dielectric properties ( $\epsilon'$  and  $\epsilon''$ ) of the selected samples as a function of the  
53  
54 temperature were measured in a microwave resonant cavity around the frequency of  
55  
56 2.45 GHz.<sup>20</sup> The methodology is based on the dynamic measurement of the  
57  
58  
59  
60

1  
2  
3 microwave cavity parameters as the resonant frequency and quality factor while with  
4  
5 the sample is being heated also with microwave energy. The heating of the sample in  
6  
7 the cavity modify the resonance properties of the microwave cavity and these changes  
8  
9 are measured to quantify the dielectric properties as a function of the temperature. An  
10  
11 automatic procedure adjusts dynamically the microwave power deliver to the  
12  
13 microwave cavity to obtain the desired heating rate in the sample. The sample  
14  
15 temperature is continuously measured with an infrared pyrometer (Optris, LT-CF2).  
16  
17 Powders were placed in a cylindrical quartz vial ( $L=15$  mm,  $\varnothing_{in}=12$  mm), manually  
18  
19 compacted to obtain a constant bed density, and immersed inside the cavity in a  $N_2$   
20  
21 atmosphere. The heating rate was adjusted to a standard rate of  $10^\circ\text{C}/\text{min}$ .  
22  
23  
24  
25  
26

## 27 **Results and Discussion**

### 28 *Characterization of pristine mesoporous silica MCM-48*

29  
30 Thirteen different batches of MCM-48 were synthesized as described above and  
31  
32 characterized by  $N_2$  adsorption (as shown in Table 1, Supplementary Info) and TEM.  
33  
34 All the samples, except one, show the same Type IV isotherm with a good  
35  
36 reproducibility giving average  $1287\pm 93$   $\text{m}^2/\text{g}$  BET surface area and  $1.011\pm 0.007$   
37  
38  $\text{cm}^3/\text{g}$  pore volume and pore size analyzed by DFT of 3.5 nm, which agrees well with  
39  
40 the values measured in the TEM images where the arrangement of the pores could be  
41  
42 observed, see Figure 2. The XRD diffraction pattern of a representative MCM-48  
43  
44 sample is presented in the bottom curve of Figure 3. It shows the typical cubic  
45  
46 structure (see Figure 1a)) indexed in the space group Ia3d. The sharp and high  
47  
48 diffraction peaks, indicate the formation of well-ordered mesoporous material.<sup>27</sup>  
49  
50  
51  
52  
53  
54  
55  
56  
57  
58  
59  
60

1  
2  
3 *Characterization of mono-, di-, tri-amine functionalized MCM-48 sorbents*

4  
5 The above-described MCM-48 material was functionalized with different silane  
6  
7 coupling agents, as schematized in Figure 1. The silane agent is covalently bond to  
8  
9 the hydroxyl groups in the silica support through alkyl-silyl linkages, see Figure 1b-c.  
10  
11 As a consequence, the textural properties of the functionalized samples are  
12  
13 considerably different from the pristine MCM-48 material, as shown by the N<sub>2</sub>  
14  
15 isotherms and pore size distributions presented in Figure 4a,b (main characterization  
16  
17 data are summarized in Table 1). MCM-48 shows a typical reversible type IV  
18  
19 adsorption isotherm (Figure 4a), which is characteristic of mesoporous materials.  
20  
21 With successive functionalization, the surface area and the pore volume are  
22  
23 significantly reduced compared to the non-functionalized MCM-48. This effect is  
24  
25 more dramatic in the case of the MCM-48-di and MCM-48-tri where bigger silane  
26  
27 molecules were grafted (see dimensions in Figure 1b). Thus, for the case of the  
28  
29 MCM-48-tri sample, the surface area has been reduced to about one third of the initial  
30  
31 BET surface, and the pore volume to about one fourth. At the same time, the pore size  
32  
33 progressively decreases from 3.5 nm in the pristine material to about 2.5 nm in the  
34  
35 MCM-48-tri sample. The amine loading based on the TGA analyses (see Figure 2  
36  
37 supplementary information) increases strongly for the case of the MCM-48-di (4.44  
38  
39 mmol N/g) compared to MCM-48-mono (1.77 mmol N/g). However, the N loading  
40  
41 obtained for MCM-48-tri (4.85 mmol N/g) is only 10% larger compared to MCM-48-  
42  
43 di (4.44 mmol N/g). This is due to a lower loading of the tri-amine silane (total weight  
44  
45 loss in the 403-1073 K interval was 22.8%, compared to 21.7% for MCM-48-di), due  
46  
47 to the steric effects experienced by this large molecule (length=1.65 nm) on the 3.5  
48  
49 nm pores of the MCM-48. The XRD analysis, see Figure 3, showed that  
50  
51 functionalization caused an apparent loss of crystallinity when compared to the non-  
52  
53  
54  
55  
56  
57  
58  
59  
60

1  
2  
3 functionalized MCM-48, especially in the case of the di-amino and tri-amino samples.  
4  
5 Kim et al.<sup>28</sup> reported that the case of M41S family materials, the peak intensity is a  
6  
7 function of the scattering contrast between the silica walls and the pore channels, and  
8  
9 this intensity decreases after grafting the organic groups to the pore surface.  
10  
11 Therefore, the decrease of the XRD peak intensity is probably due to the grafting the  
12  
13 organic groups, rather than to a loss of structure. Similar changes have been reported  
14  
15 with previous studies of functionalization of mesoporous silica.<sup>24,28</sup>  
16  
17 FTIR spectra of the samples are presented in Figure 5. The peak at the 3743 cm<sup>-1</sup> is  
18  
19 assigned to single Si-OH, and this band completely disappeared in the functionalized  
20  
21 MCM-48 samples, which indicates that all single Si-OH groups were covalently  
22  
23 attached through siloxane Si-O-Si bonds with the silane agent. The grafting was also  
24  
25 confirmed by the appearance of absorption peaks of N-H bonds (3368-3298 cm<sup>-1</sup> and  
26  
27 1590-1478cm<sup>-1</sup>) and C-H bonds (2931-2869cm<sup>-1</sup>) consistent with the functional  
28  
29 groups used.<sup>28-30</sup>  
30  
31  
32  
33  
34

### 35 *Dielectric Properties and microwave heating*

36  
37 The dielectric constant ( $\epsilon'$ ), dielectric loss ( $\epsilon''$ ) and the loss tangent ( $\tan\delta$ ) are  
38  
39 presented in Figure 6(a,b) as a function of temperature. 473 K was chosen as the  
40  
41 maximum temperature for these tests following the results of the TGA analysis (see  
42  
43 supplementary information) indicating that above this temperature a significant  
44  
45 degradation of the functional groups could take place. Figure 6 shows that increasing  
46  
47 the concentration of amino groups increased the dielectric constant and dielectric loss  
48  
49 compared to non-functionalized MCM-48 samples. The increase in the dielectric  
50  
51 constant is related to higher density of N-H dipoles (see Figure 1b, c) that can move  
52  
53 freely in the grafted molecules. The loss tangent (Figure 6b), shows the efficiency of  
54  
55 MW energy conversion into heat. In the case of MCM-48, this value decreases with  
56  
57  
58  
59  
60

1  
2  
3 temperature in the entire interval studied. For this material, as the temperature  
4 increases, the condensation of the polar O-H groups on the silica surface takes place  
5 and after 100°C, most of them have disappeared and the value of loss tangent is  
6 negligible indicating that this material has a very low capacity to absorb microwave  
7 energy. However, in the case of the amino-grafted materials as the number of N-H  
8 groups increases, the loss tangent increases. The loss tangent values correlate  
9 perfectly with the heating experiments under microwave shown in Figure 7. In this  
10 experiment, three slabs of amino modified materials were placed together inside the  
11 microwave cavity, and the temperature of the surface of the slabs was recorded with  
12 an IR camera, (see Figure 7a). After the samples were allowed to reach a steady  
13 temperature, a clear temperature difference could be observed. The samples with  
14 lower amino group content and thus lower loss tangent presented the lowest  
15 temperature. The same effect could be observed by following the temperature inside a  
16 fixed-bed packed with the different powders and heated in the microwave cavity  
17 (Figure 7b). Again, the MCM-48-tri heated more intensely, reaching 413 K in 3 min,  
18 a temperature well above that required for the regeneration amino functionalized  
19 materials exposed to CO<sub>2</sub>, as will be shown below.  
20  
21  
22  
23  
24  
25  
26  
27  
28  
29  
30  
31  
32  
33  
34  
35  
36  
37  
38  
39  
40

#### 41 *CO<sub>2</sub> adsorption*

42  
43 Figure 8 shows CO<sub>2</sub> adsorption isotherms at 298 K for the different samples. As could  
44 be expected, for the same partial pressure the amount of CO<sub>2</sub> adsorbed increases as  
45 the density of amino groups increases. In the case of MCM-48-mono with an amine  
46 load of 1.77 mmol N/g a maximum CO<sub>2</sub> adsorption around 1 mmol CO<sub>2</sub>/g could be  
47 achieved, a value that agrees well with previous data on the same material.<sup>24</sup> In the  
48 case of MCM-48-di and tri, there a sharp increase in the isotherm can be observed at  
49 low partial pressure of CO<sub>2</sub>, corresponding to a Langmuir type I isotherm, indicating  
50  
51  
52  
53  
54  
55  
56  
57  
58  
59  
60

1  
2  
3 that chemisorption takes place. For the MCM-48-di and tri samples a load around 0.3  
4 mmol CO<sub>2</sub>/mmol N at 5kPa of CO<sub>2</sub> was achieved, see Table 1.

5  
6  
7 Chang et al.<sup>29</sup> reported that the reaction of CO<sub>2</sub> with amino groups under dry and  
8 humid conditions results in the formation of carbamates, giving a ratio of 0.5 mmol  
9 CO<sub>2</sub>/mmol N for -mono and -di and 0.66 mmol CO<sub>2</sub>/mmol N for -tri. This means that  
10 there is still considerable room for optimization of the grafting procedure in our  
11 samples that could lead to further increases in CO<sub>2</sub> loading.  
12  
13  
14  
15  
16  
17

### 18 *Thermal and microwave regeneration of sorbents*

19  
20 The CO<sub>2</sub> desorption curves under conventional and microwave heating are presented  
21 in Figure 9(a,b), together with the evolution of temperature and normalized  
22 occupancy (Figure 9c) of the sorbent. The kinetic analysis<sup>19</sup> showed that, even though  
23 under conventional heating the highest available heating ramp was attempted  
24 (20K/min) desorption using microwave heating is approximately 4 times faster.  
25 Again, it can be seen that the MCM-48-tri sample present the fastest heating (and  
26 fastest) regeneration of the three amino-functionalized samples.  
27  
28  
29  
30  
31  
32  
33  
34  
35  
36

37 Finally, to test the stability and the regenerability of solid sorbents under microwave  
38 heating, a series of cyclic experiments involving CO<sub>2</sub> adsorption at room temperature  
39 and desorption under microwave heating were performed with mono-, di- and tri-  
40 amine functionalized MCM-48 samples (Figure 10). The average CO<sub>2</sub> uptakes in 20  
41 cycles (except di-, only 8 cycles) for mono, di- and tri- amine functionalized samples  
42 were 0.2±0.02, 1.23±0.07 and 1.59 ± 0.10 mmol CO<sub>2</sub>/g sorbent, respectively. It can  
43 be seen that the stability was excellent, with no apparent loss of adsorption capacity  
44 after 20 cycles. The stability can be attributed to the chemical grafting of the amino  
45 groups on the silica surface, giving a clear advantage to these materials over amine-  
46 impregnated silica where amine leaching (and the subsequent loss of capacity) is  
47  
48  
49  
50  
51  
52  
53  
54  
55  
56  
57  
58  
59  
60



1  
2  
3 common.<sup>31</sup> With grafted molecules, the behavior is highly stable unless conditions are  
4  
5 strong enough to break covalent bonds, giving covalently tethered amine adsorbents  
6  
7 the potential to be subjected to repeated adsorption and desorption cycles<sup>32</sup> as shown  
8  
9 in Figure 10.  
10

## 11 **Conclusions**

12  
13 The dielectric characterization measurements show that the incorporation of amino  
14  
15 groups on otherwise low-interaction supports such as silica, enables polarization by  
16  
17 the electromagnetic field and strongly enhances response in the microwave frequency  
18  
19 range. This result in direct heating of the surface of amino-grafted silica, accelerating  
20  
21 temperatures rise and desorption of adsorbed species. The advantages for sorbent  
22  
23 regeneration are substantial since energy is directly transferred to the solid in a highly  
24  
25 efficient way, and also because the accelerated desorption facilitates the production of  
26  
27 a highly concentrated exit stream.  
28  
29

30  
31 The MWSA process using amino-functionalized materials seems especially apt for  
32  
33 CO<sub>2</sub> capture systems. Increasing the concentration of amino groups (by grafting  
34  
35 mono, di- and tri-amine molecules) simultaneously increases CO<sub>2</sub> adsorption at low  
36  
37 ambient partial pressures and the response under MW heating at 2.45 GHz, leading to  
38  
39 a fast (approximately 4 times faster than conventional heating under the conditions  
40  
41 studied) regeneration. Furthermore, chemical grafting produces a stable material  
42  
43 under MWSA conditions: no effect was observed on the adsorption capacity after 20  
44  
45 adsorption-regeneration cycles.  
46  
47  
48  
49  
50  
51  
52  
53  
54  
55  
56  
57  
58  
59  
60

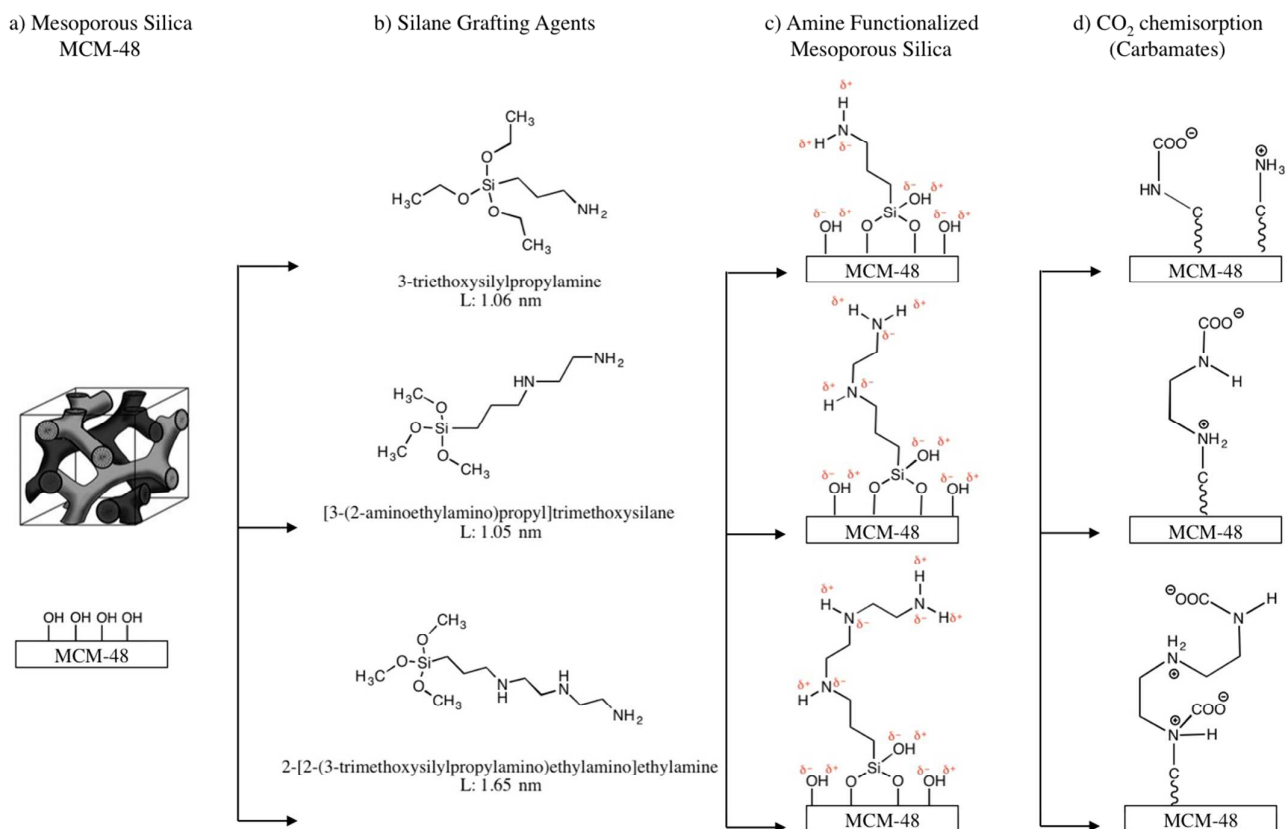
1  
2  
3 *Acknowledgments*  
4

5 Financial support from the European Research Council ERC-Advanced Grant HECTOR  
6  
7 is gratefully acknowledged. Hakan Nigar also acknowledges financial support from the  
8  
9 Spanish Ministry of Education for the FPU grant (Formación del Profesorado  
10  
11 Universitario – FPU12/06864).  
12  
13  
14  
15  
16  
17  
18  
19  
20  
21  
22  
23  
24  
25  
26  
27  
28  
29  
30  
31  
32  
33  
34  
35  
36  
37  
38  
39  
40  
41  
42  
43  
44  
45  
46  
47  
48  
49  
50  
51  
52  
53  
54  
55  
56  
57  
58  
59  
60

For peer review only

## FIGURES

Figure 1 – Schematic view of the covalent bonding through the alkyl-silyl linkages and formation of carbamates<sup>29</sup>.



- ChemDraw Professional v.15 was used for drawing the molecules.
- Schematized figure of MCM-48 was adapted from: Mesosilica materials and organic pollutant adsorption: part A removal from air , DOI: 10.1039/c3cs60096c

Figure 2 – TEM images of pristine MCM-48 sample after calcination

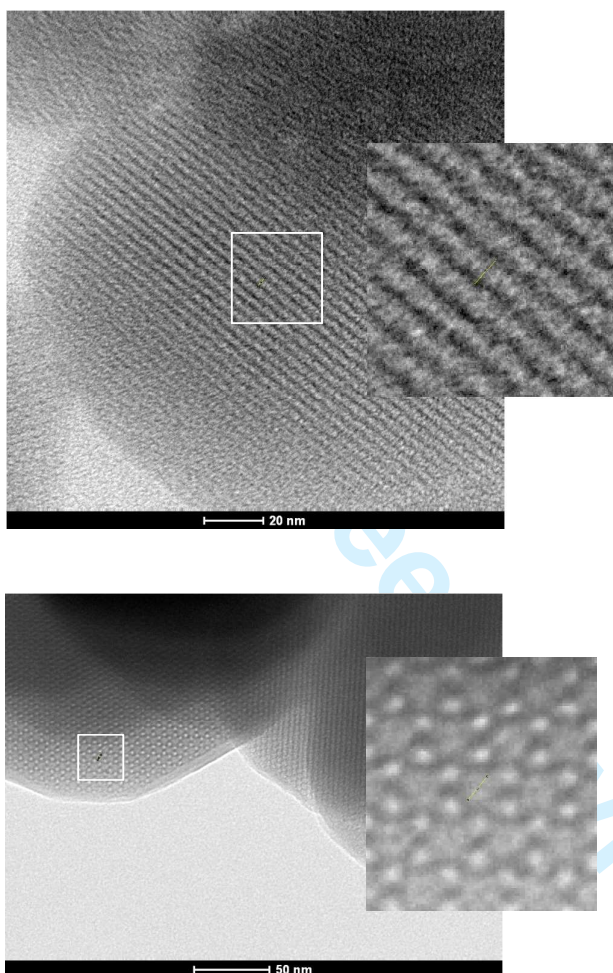


Figure 3 – XRD patterns of non-functionalized and functionalized MCM-48 samples

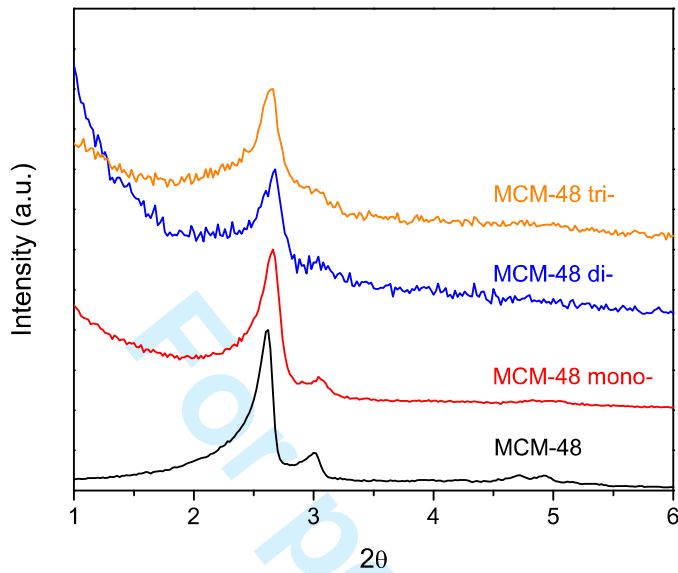
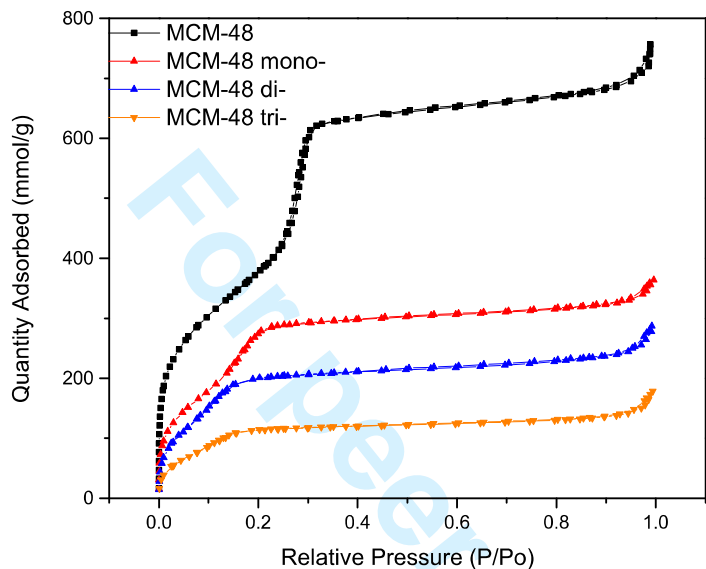


Figure 4 – (a) N<sub>2</sub> adsorption-desorption isotherms and (b) pores size distribution of non-functionalized and functionalized MCM-48 samples

a)



b)

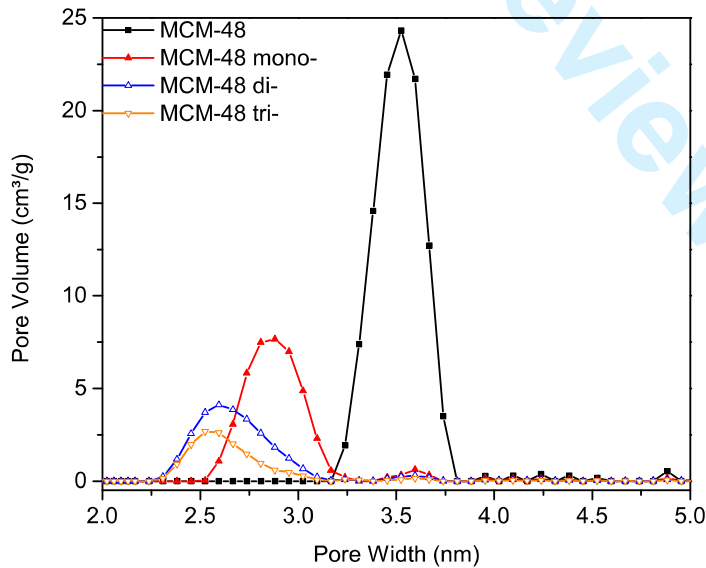


Figure 5 – FTIR spectrum of non-functionalized and functionalized MCM-48 samples

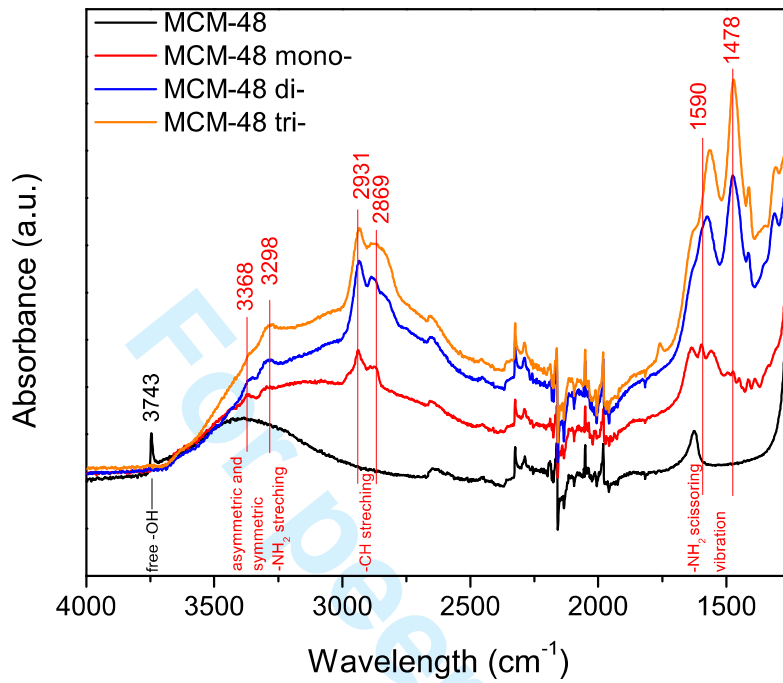
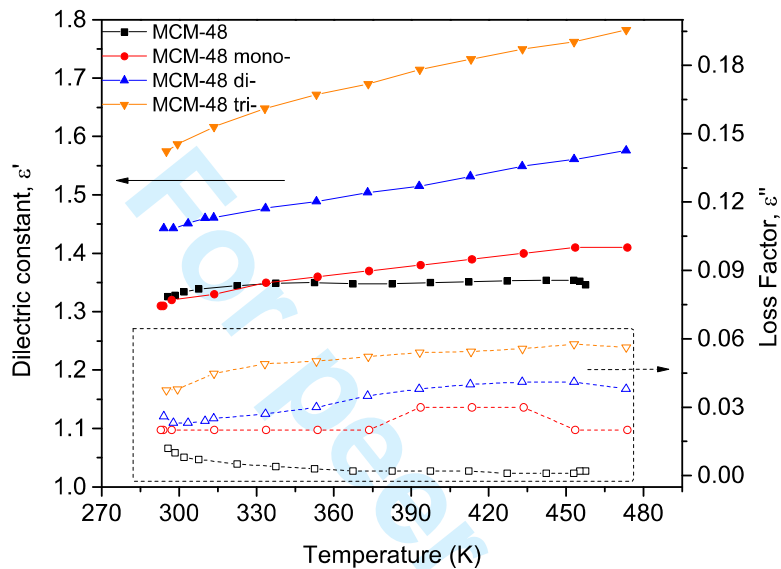
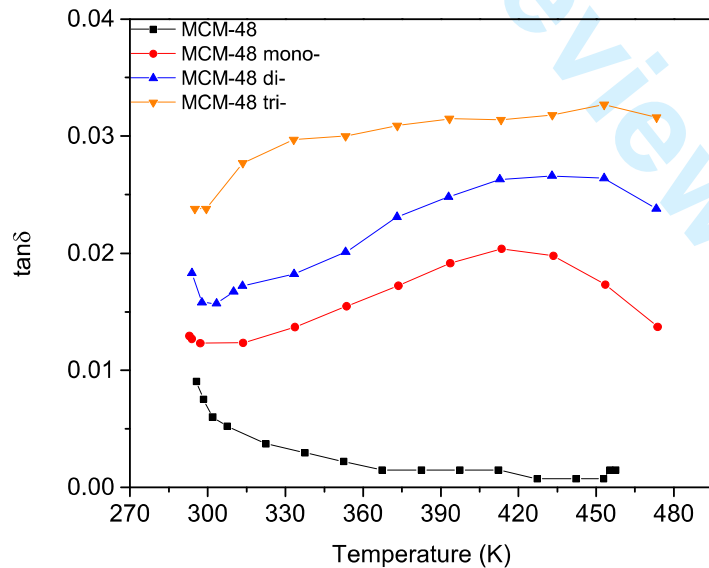


Figure 6 – Dielectric Properties, a) dielectric constant and loss factor, b) loss tangent as a function of temperature

a)



b)





1  
2  
3 Figure 7 – a) Surface temperature, measure with thermographic camera of functionalized samples  
4 heated inside the MW cavit, 5W. b) Temperature vs. time in fixed-bed of the different samples,  
5  
6  
7 m=100 mg, 60W. Temperature measured with an optical fiber located inside the bed  
8  
9  
10  
11  
12  
13  
14  
15  
16  
17  
18  
19  
20  
21  
22  
23  
24  
25  
26  
27  
28  
29  
30  
31  
32  
33  
34  
35  
36  
37  
38  
39  
40  
41  
42  
43  
44  
45  
46  
47  
48  
49  
50  
51  
52  
53  
54  
55  
56  
57  
58  
59  
60

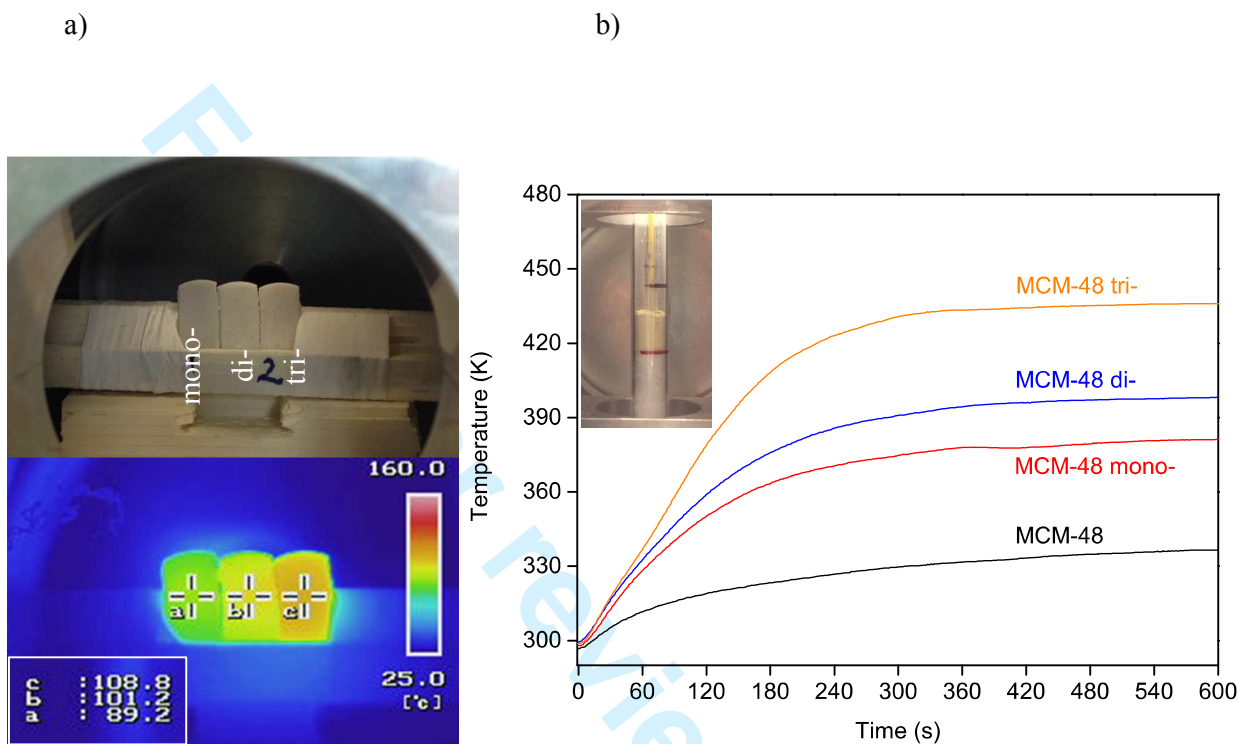


Figure 8 – CO<sub>2</sub> adsorption isotherms at 298 K for non-functionalized and functionalized MCM-48 samples

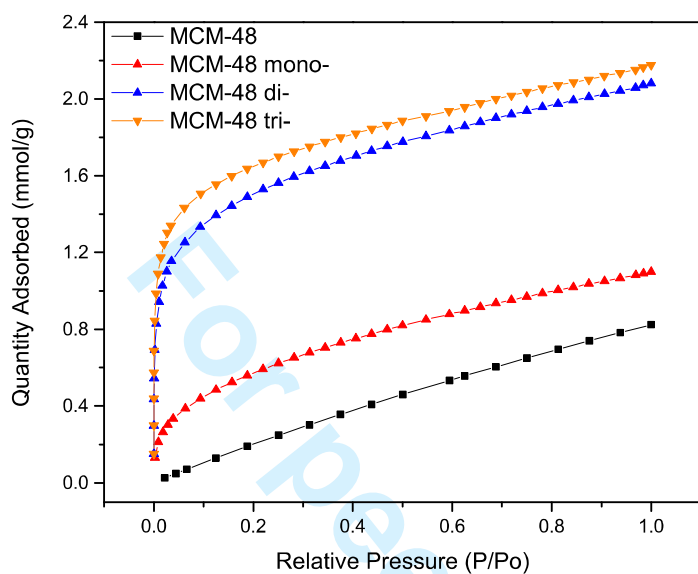
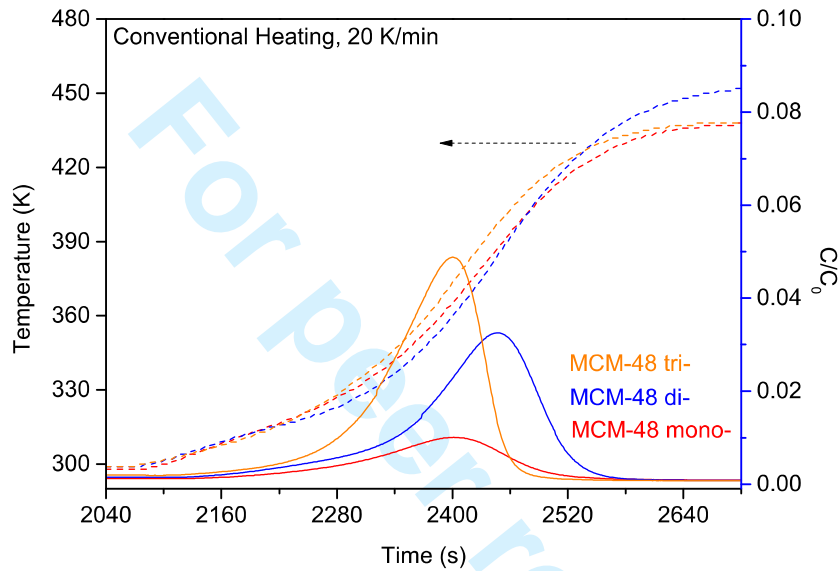
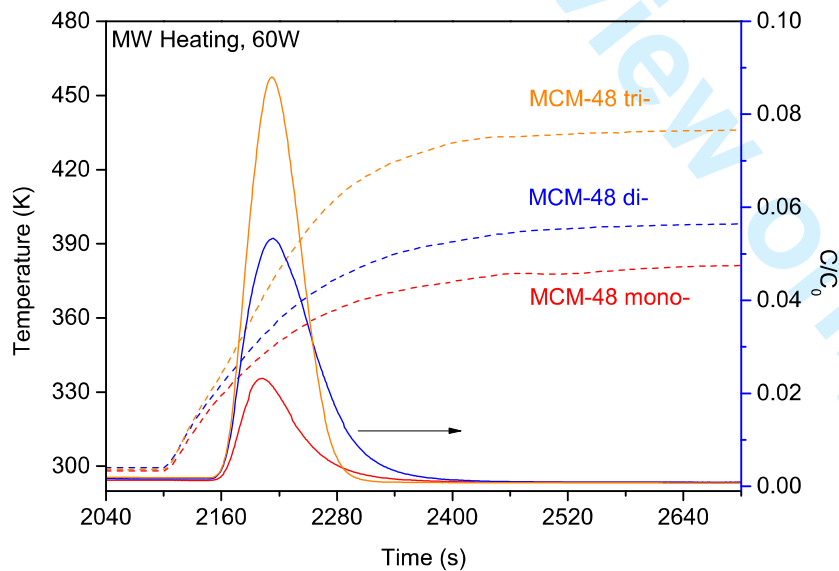


Figure 9 – Evolution of temperature and normalized concentration during a) conventional and b) MW regeneration of sorbents saturated with CO<sub>2</sub> at 1 bar 298 K. c) Occupancy vs. Time for conventional and MW heating

a)



b)



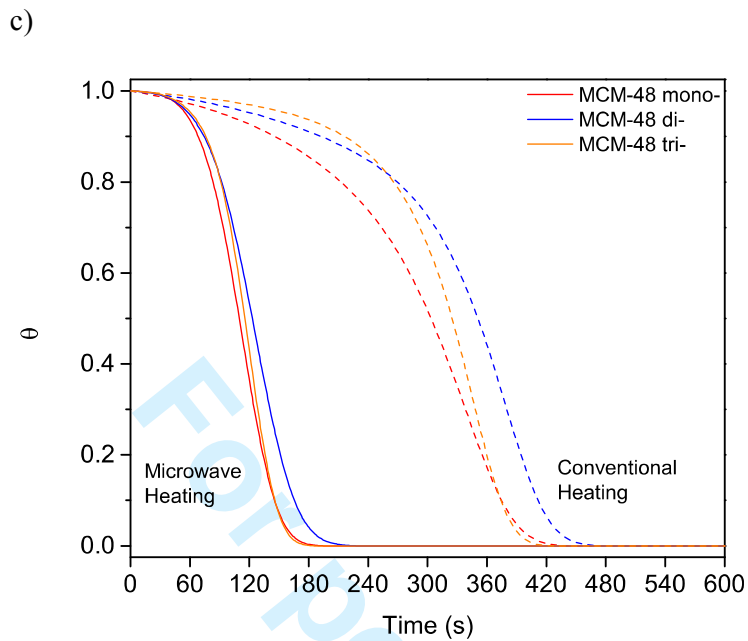
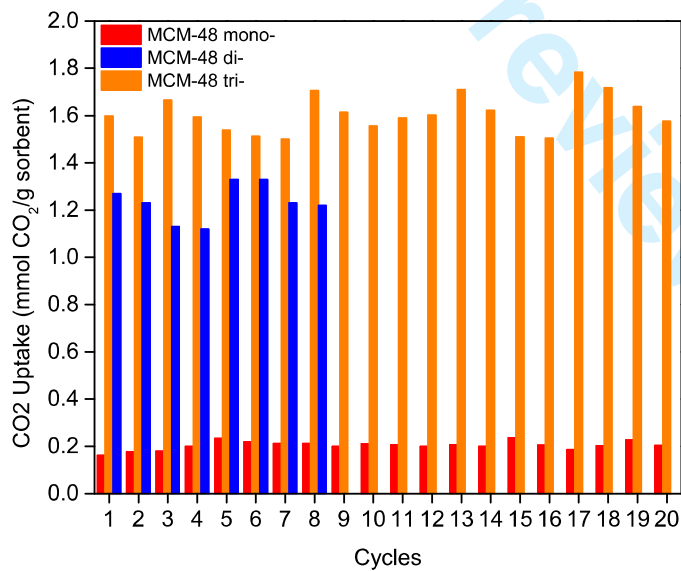


Figure 10 – Cyclic adsorption of CO<sub>2</sub>



## TABLES

Table 1 – Textural properties and CO<sub>2</sub> uptake extracted from N<sub>2</sub> and CO<sub>2</sub> isotherms of MCM-48 samples with varying degrees of amine functionalization

Sample	BET Surface Area	Pore Volume	Pore Size	mmol N/g	mmol CO <sub>2</sub> /mmol N @5 kPa	mmol CO <sub>2</sub> /mmol N @101 kPa
	m <sup>2</sup> /g	cm <sup>3</sup> /g	nm			
MCM-48	1287	1.11	3.5	-	-	-
MCM-48 mono-	1072	0.52	2.9	1.77	0.22	0.62
MCM-48 di-	698	0.39	2.6	4.44	0.27	0.46
MCM-48 tri-	463	0.23	2.5	4.85	0.31	0.44

## REFERENCES

1. Boot-Handford ME, Abanades JC, Anthony EJ, et al. Carbon capture and storage update. *Energy and Environmental Science*. 2014;7(1):130-189.
2. Goepfert A, Czaun M, Surya Prakash GK, Olah GA. Air as the renewable carbon source of the future: An overview of CO<sub>2</sub> capture from the atmosphere. *Energy and Environmental Science*. 2012;5(7):7833-7853.
3. Mason JA, Sumida K, Herm ZR, Krishna R, Long JR. Evaluating metal-organic frameworks for post-combustion carbon dioxide capture via temperature swing adsorption. *Energy and Environmental Science*. 2011;4(8):3030-3040.
4. Harlick PJE, Sayari A. Applications of pore-expanded mesoporous silica. 5. triamine grafted material with exceptional CO<sub>2</sub> dynamic and equilibrium adsorption performance. *Industrial and Engineering Chemistry Research*. 2007;46(2):446-458.
5. Franchi RS, Harlick PJE, Sayari A. Applications of pore-expanded mesoporous silica. 2. Development of a high-capacity, water-tolerant adsorbent for CO<sub>2</sub>. *Industrial and Engineering Chemistry Research*. 2005;44(21):8007-8013.
6. Webley PA, Zhang J. Microwave assisted vacuum regeneration for CO<sub>2</sub> capture from wet flue gas. *Adsorption*. 2014;20(1):201-210.
7. Stankiewicz A. On the Applications of Alternative Energy Forms and Transfer Mechanisms in Microprocessing Systems. *Industrial & Engineering Chemistry Research*. 2007/06/01 2007;46(12):4232-4235.
8. Clark DE, Folz DC, West JK. Processing materials with microwave energy. *Materials Science and Engineering: A*. 8/15/ 2000;287(2):153-158.
9. Chandrasekaran S, Ramanathan S, Basak T. Microwave material processing-a review. *AIChE Journal*. 2012;58(2):330-363.
10. Borrell A, Salvador MD, Miranda M, Penaranda-Foix FL, Catala-Civera JM. Microwave technique: A powerful tool for sintering ceramic materials. *Current Nanoscience*. 2014;10(1):32-35.
11. Durka T, van Gerven T, Stankiewicz A. Microwaves in heterogeneous gas-phase catalysis: Experimental and numerical approaches. *Chemical Engineering and Technology*. 2009;32(9):1301-1312.
12. Cherbański R, Molga E. Intensification of desorption processes by use of microwaves-An overview of possible applications and industrial perspectives. *Chemical Engineering and Processing: Process Intensification*. // 2009;48(1):48-58.
13. Hashisho Z, Rood MJ, Barot S, Bernhard J. Role of functional groups on the microwave attenuation and electric resistivity of activated carbon fiber cloth. *Carbon*. 2009;47(7):1814-1823.
14. Menéndez JA, Arenillas A, Fidalgo B, et al. Microwave heating processes involving carbon materials. *Fuel Processing Technology*. 1// 2010;91(1):1-8.
15. Çalışkan E, Bermúdez JM, Parra JB, Menéndez JA, Mahramanlioğlu M, Ania CO. Low temperature regeneration of activated carbons using microwaves: Revising conventional wisdom. *Journal of Environmental Management*. 2012;102:134-140.

16. Ohgushi T, Komarneni S, Bhalla AS. Mechanism of microwave heating of zeolite A. *Journal of Porous Materials*. 2001;8(1):23-35.
17. Legras B, Polaert I, Estel L, Thomas M. Mechanisms responsible for dielectric properties of various faujasites and linde type A zeolites in the microwave frequency range. *Journal of Physical Chemistry C*. // 2011;115(7):3090-3098.
18. Gracia J, Escuin M, Mallada R, Navascues N, Santamaría J. Heating of zeolites under microwave irradiation: A density functional theory approach to the ion movements responsible of the dielectric loss in Na, K, and Ca A-zeolites. *Journal of Physical Chemistry C*. // 2013;117(30):15659-15666.
19. Nigar H, Navascués N, De La Iglesia O, Mallada R, Santamaría J. Removal of VOCs at trace concentration levels from humid air by Microwave Swing Adsorption, kinetics and proper sorbent selection. *Separation and Purification Technology*. 2015;151:193-200.
20. Catala-Civera JM, Canos AJ, Plaza-Gonzalez P, Gutierrez JD, Garcia-Banos B, Penaranda-Foix FL. Dynamic Measurement of Dielectric Properties of Materials at High Temperature During Microwave Heating in a Dual Mode Cylindrical Cavity. *Microwave Theory and Techniques, IEEE Transactions on*. 2015;63(9):2905-2914.
21. Belmabkhout Y, Sayari A. Isothermal versus non-isothermal adsorption-desorption cycling of triamine-grafted pore-expanded MCM-41 mesoporous silica for CO<sub>2</sub> capture from flue gas. *Energy and Fuels*. 2010;24(9):5273-5280.
22. Chowdhury T, Shi M, Hashisho Z, Kuznicki SM. Indirect and direct microwave regeneration of Na-ETS-10. *Chemical Engineering Science*. 5/24/2013;95:27-32.
23. Chronopoulos T, Fernandez-Diez Y, Maroto-Valer MM, Ocone R, Reay DA. CO<sub>2</sub> desorption via microwave heating for post-combustion carbon capture. *Microporous and Mesoporous Materials*. 10// 2014;197:288-290.
24. Gil M, Tiscornia I, de la Iglesia Ó, Mallada R, Santamaría J. Monoamine-grafted MCM-48: An efficient material for CO<sub>2</sub> removal at low partial pressures. *Chemical Engineering Journal*. // 2011;175(1):291-297.
25. Sayari A, Heydari-Gorji A, Yang Y. CO<sub>2</sub>-induced degradation of amine-containing adsorbents: Reaction products and pathways. *Journal of the American Chemical Society*. 2012;134(33):13834-13842.
26. Jaroniec M, Kruk M, Olivier JP, Koch S. A new method for the accurate pore size analysis of MCM-41 and other silica based mesoporous materials. *Studies in Surface Science and Catalysis*. Vol 1282000:71-80.
27. Schumacher K, Ravikovitch PI, Du Chesne A, Neimark AV, Unger KK. Characterization of MCM-48 Materials. *Langmuir : the ACS journal of surfaces and colloids*. 2000/05/01 2000;16(10):4648-4654.
28. Kim S, Ida J, Gulians VV, Lin JYS. Tailoring pore properties of MCM-48 silica for selective adsorption of CO<sub>2</sub>. *Journal of Physical Chemistry B*. 2005;109(13):6287-6293.
29. Chang F-Y, Chao K-J, Cheng H-H, Tan C-S. Adsorption of CO<sub>2</sub> onto amine-grafted mesoporous silicas. *Separation and Purification Technology*. 11/19/2009;70(1):87-95.
30. Bacsik Z, Ahlsten N, Ziadi A, et al. Mechanisms and kinetics for sorption of CO<sub>2</sub> on bicontinuous mesoporous silica modified with n-propylamine. *Langmuir : the ACS journal of surfaces and colloids*. Sep 6 2011;27(17):11118-11128.

- 1
  - 2
  - 3
  - 4
  - 5
  - 6
  - 7
  - 8
  - 9
  - 10
  - 11
  - 12
  - 13
  - 14
  - 15
  - 16
  - 17
  - 18
  - 19
  - 20
  - 21
  - 22
  - 23
  - 24
  - 25
  - 26
  - 27
  - 28
  - 29
  - 30
  - 31
  - 32
  - 33
  - 34
  - 35
  - 36
  - 37
  - 38
  - 39
  - 40
  - 41
  - 42
  - 43
  - 44
  - 45
  - 46
  - 47
  - 48
  - 49
  - 50
  - 51
  - 52
  - 53
  - 54
  - 55
  - 56
  - 57
  - 58
  - 59
  - 60
31. Chen C, Yang S-T, Ahn W-S, Ryoo R. Amine-impregnated silica monolith with a hierarchical pore structure: enhancement of CO<sub>2</sub> capture capacity. *Chemical Communications*. 2009(24):3627-3629.
32. Choi S, Drese JH, Jones CW. Adsorbent Materials for Carbon Dioxide Capture from Large Anthropogenic Point Sources. *ChemSusChem*. 2009;2(9):796-854.

For peer review only